Drug Design, Development and Therapy

Dovepress

open access to scientific and medical research

Open Access Full Text Article

ORIGINAL RESEARCH

Integrating Network Pharmacology and Experimental Validation to Decipher the Mechanism of Action of Huanglian Jiedu Decoction in Treating Atherosclerosis

Jiahua Liang[1,*]
Yingjie Huang[1,*]
Zhexing Mai[1,*]
Qunzhang Zhan[1]
Hengchen Lin[1]
Yuxin Xie[1]
Haihao Wang[1]
Yan Liu[1]
Chuanjin Luo[2]

[1]The First Clinical Medical College, Guangzhou University of Chinese Medicine, Guangzhou, Guangdong, People's Republic of China; [2]The Department of Cardiovascular Disease, Guangzhou University of Traditional Chinese Medicine First Affiliated Hospital, Guangzhou, Guangdong, People's Republic of China

*These authors contributed equally to this work

Correspondence: Chuanjin Luo
The Department of Cardiovascular Disease, Guangzhou University of Traditional Chinese Medicine First Affiliated Hospital, Jichang Road 16#, District Baiyun, Guangzhou, 510405, Guangdong, People's Republic of China
Email Gztcm1964@163.com

Background: This study used network pharmacology, molecular docking and experimental validation to assess the effects of Huanglian Jiedu Decoction (HLJDD) on atherosclerosis (AS).

Methods: The components and targets of HLJDD were analyzed using the Traditional Chinese Medicine Systems Pharmacology database, and information on the genes associated with AS was retrieved from the GeneCards and OMIM platforms. Protein–protein interactions were analyzed using the STRING platform. A component–target–disease network was constructed using Cytoscape. GO and KEGG analyses were performed to identify molecular biological processes and signaling pathways, and the predictions were verified experimentally. Molecular docking was conducted with ChemOffice software, PyMOL software and Vina to verify the correlation of targets and compounds.

Results: HLJDD contained 31 active compounds, with quercetin, kaempferol, moupinamide and 5-hydroxy-7-methoxy-2-(3,4,5-trimethoxyphenyl)chromone as the core compounds. The most important biotargets of HLJDD in AS were ICAM-1, CD31 and RAM-11. The molecular docking results showed that the molecular docking interaction energy between the 3 key targets and the 4 high-degree components were much less than -5 kJ·mol^{-1}. The experimental validation results showed that HLJDD might treat AS mainly by reducing TC, TG and LDL-C and increasing HDL-C, upregulating CD31 expression, reducing ICAM-1 and RAM-11 expression, and downregulating inflammatory factors, including CRP, IL-6 and TNF-α. These results support the network pharmacology data and demonstrate that HLJDD affects the expression of core genes and alters the leukocyte transendothelial migration signaling pathway.

Conclusion: Based on network pharmacology and experimental validation, our study indicated that HLJDD exerted anti-AS effect through upregulating CD31 expression and reducing the expression of ICAM-1 and RAM-11. HLJDD may be a potential therapeutic drug to the prevention of AS.

Keywords: Huanglian Jiedu Decoction, atherosclerosis, network pharmacology, molecular docking, experimental validation

Introduction

Atherosclerosis (AS) is an inflammatory process initiated by subendothelial retention of lipids. The unstable plaques formed by lipids can trigger cardiovascular disease (CVD), making AS a principal source of cardiovascular mortality.[1] At

present, AS is mainly treated by blocking cholesterol ester synthesis and antiplatelet activity. However, medicines that block the cholesterol synthesis and the antiplatelet activity have obvious side effects.[2–4] In addition, it has been confirmed that inhibition of the inflammatory response is a potential pathway to intervene in AS.[5] Over the past two thousand years, traditional Chinese medicine (TCM) has been widely used in China and other Asian countries. As one of the most popular supplements and alternative medicines in the world, TCM has been gradually accepted by non-Chinese individuals because of its prominent efficacy, abundant resources, and low toxicity. In TCM, there are many theories according to the pathogenesis of AS, such as damp heat (Shi-re in Chinese), phlegm stasis (Tan-yu in Chinese), and toxic pathogen (Du-xie in Chinese). It means that the treatment principles of clearing away heat, removing dampness and detoxicating would be effective for AS.[6]

Huanglian Jiedu Decoction (HLJDD) is a traditional Chinese medicine prescription comprising Coptidis Rhizoma (Huang-lian in Chinese), Scutellariae Radix (Huang-qin in Chinese), Phellodendri Chinensis Cortex (Huang-bo in Chinese) and Gardeniae Fructus (Zhi-zi in Chinese). HLJDD had been used for 1700 years in China and was mainly depending on clearing away heat-toxin to intervene in the inflammatory disorder, the basic pathophysiological process of AS.[6] Recent studies have shown that HLJDD has obvious anti-inflammatory, antibacterial and other pharmacological effects. Additionally, HLJDD protects myocardial cells by lowering blood lipids and blood pressure and demonstrating anti-atherosclerosis, anti-arrhythmia and anti-thrombosis activities.[7] HLJDD may inhibit the occurrence and development of AS by affecting the functional differentiation of some immune cells.[8] Therefore, HLJDD may be a feasible treatment considering the pharmacological mechanisms.

TCM is a complex system with hundreds of pharmacological compounds.[9] Unlike Western medicine, the theory of TCM emphasizes the integrity of the entire human body. Because of the complexity of its composition, it is difficult to systematically investigate the molecular mechanism of action of herbs. Network pharmacology is a new subject based on the theory of systems biology, pharmacokinetic and pharmacodynamic properties of drugs as well as protein targets and their pharmacological activities, which analyzes the network of biological systems and selects specific signal nodes to perform multi-target drug molecular design.[10] Network pharmacology offers a new approach to the study of Chinese medicine, demonstrating the advantages of multi-compound, multi-target and multi-pathway features of Chinese medicine prescriptions and providing a systematic solution for Chinese medicine prescription research from quality control to clinical efficacy.[11]

In the current study, we used computational resources to construct the pharmacological network of HLJDD in AS to predict the active compounds and potential protein targets and pathways. The results showed that HLJDD contained 31 active compounds, with quercetin, kaempferol, moupinamide and 5-hydroxy-7-methoxy-2-(3,4,5-trimethoxyphenyl)chromone as the core compounds. The most important biotargets of HLJDD in AS were ICAM-1, CD31 and RAM-11. The molecular docking results showed that the molecular docking interaction energy between the 3 key targets and the 4 high-degree components were much less than -5 kJ·mol^{-1}. The experimental validation results showed that HLJDD significantly influenced the expression of the 3 targets predicted by network pharmacology.

Materials and Methods

Collection of Chemical Components and Targets of HLJDD

To evaluate the pharmacokinetics of HLJDD, we used the TCMSP database (http://lsp.nwu.edu.cn/) to collect information about the chemical composition of HLJDD. The TCMSP database is a systematic pharmacological resource to evaluate Chinese medicines or related compounds.[12] Using the pharmacokinetic information retrieval filter based on the TCMSP platform, the oral bioavailability (OB) and drug-likeness (DL) can be set to ≥30% and ≥0.18 to obtain qualified herbal compounds.

Collection of Disease-Associated Targets

Potential genes associated with AS were collected from GeneCards (https://www.genecards.org/) and OMIM (https://www.omim.org/). GeneCards is a comprehensive and authoritative human gene integrator that assembles several descriptions about human genes from over 80 digital sources.[13] The OMIM database is also an extensive and canonical research resource for information on genes and phenotypes that is secured from peer-reviewed biomedical literature examined by more than 45 high-impact journals.[14] We gathered the AS-related targets by searching the databases mentioned above using the keyword

"atherosclerosis, atheroscleroses, atherogenesis and arteriosclerosis".

Construction of the Component–Common Target–Disease Network

Venny2.1.0 (http://bioinfogp.cnb.csic.es/tools/venny/), an interactive tool for comparing lists using Venn diagrams[15] is used to screen common potential therapeutic targets between HLJDD and AS-related targets. Cytoscape-v3.7.1, a free software for visualizing complex networks,[16] is used to build the HLJDD component–common target–AS network model for more visualized understanding of the interrelationships between them.

Protein–Protein Interaction (PPI) Data

The Search Tool for the Retrieval of Interacting Genes (STRING) database (https://string-db.org/, ver. 10.5), a database that searches for known and predicted protein-to-protein interactions,[17] was used to analyze the protein–protein interactions of the common targets of the HLJDD and AS-related targets. The database defines PPIs with confidence ranges for data scores.

GO and KEGG Enrichment Analyses

The Cytoscape plugin ("ClueGO2.5.6") was selected for the enrichment analysis of GO-BP, which supports over 200 species, real-time database updates, multiple annotated databases and network graph displays. We performed pathway enrichment analysis using the KEGG data obtained from the DAVID 6.8 platform (https://david.ncifcrf.gov/). DAVID now provides a comprehensive set of functional annotation tools for investigators to understand the underlying biological significance of a large list of genes. The P-values were calculated in these two enrichment analyses, and specific disease pathways were excluded. $P < 0.05$ indicated that the enrichment degree was statistically significant.

Molecular Docking

The 3D structure of each compound was established, the energy was minimized in ChemOffice software and the structure was saved in *mol2 format. The protein labels relevant to the top 3 targets with the highest degree values were found through the STRING database, and then their 3D structures were downloaded in *PDB format through the PDB database (https://www.rcsb.org/). PyMOL software was used to affix hydrogen atoms and remove water molecules from proteins, and the format of compounds and target proteins was transformed into *pdbqt through AutoDock software. Finally, Vina was used for docking. A binding energy less than 0 indicates that the ligand can spontaneously bind the receptor.

Experimental Verification

HLJDD Preparation

HLJDD comprising four herbal medicines (Scutellariae Radix; Phellodendri Chinensis Cortex; Coptidis Rhizome; Gardeniae Fructus) at a ratio of 6:6:9:9 was prepared by the pharmacy of the First Affiliated Hospital of Guangzhou University of Chinese Medicine (Guangzhou, China). All the herbs were extracted twice with boiling water, and the combined filtrate was concentrated to obtain the decoction (2.0 g/mL).

Animal Treatments

Forty clean and healthy male New Zealand white rabbits (three months old, 2.5–3 kg) were provided by the Animal Experimental Center of Guangzhou University of Chinese Medicine (Guangzhou, China), and they were maintained individually under a controlled specific pathogen-free environment (temperature, 23° ± 2 °C; relative humidity: 50% ± 10%; 12-hr light/dark cycle) and were fed an ordinary diet for 2 weeks. The Animal Experimental Ethics Committee of Guangzhou University of Chinese Medicine previously approved all the experimental procedures, which met the standards outlined in the Guidelines for Animal Experiments of the Chinese Medical Ethics Committee. All the relevant rules on the handling of animals were strictly followed. The rabbits were randomized into the following four groups (n=10 each): control group (Control), atherosclerotic model group (Model), conventional-dose HLJDD treatment group (HLJDD) and high-dose HLJDD treatment group (High-HLJDD). The control group was fed a normal chow diet, while the other three groups were fed a high-fat diet (1% cholesterol, 5% lard, 94% standard diet, 100 g/d, provided by the animal center of Guangzhou University of Chinese Medicine) to establish the AS model.[18] The medical dosage of rabbit were 3.35 times that used in humans. In the present study, conventional-dose HLJDD in rabbit was selected as the clinically equivalent dose of HLJDD in humans (HLJDD clinical dose: 30 g/day, adult weight 70 kg, the dose of rabbit was: 30 g/70 kg × 3.35 ≈ 1.5 g/kg). High-dose HLJDD were twice times of the equivalent doses in rabbit. After 12 weeks of continuous feeding, the

conventional-dose HLJDD treatment group received 1.5 g/kg/d of HLJDD, while the high-dose HLJDD treatment group received 3 g/kg/d of HLJDD. All the treatments were delivered by oral gavage for 12 weeks. At the end of the experimental period, all the rabbits were euthanized. The animal experiments were approved by The Animal Ethics Committee of Guangzhou University of Chinese Medicine (Guangzhou, China).

Measurement of Blood Lipids

The plasma concentrations of TC, TG, LDL-c, and HDL-c were detected according to manufacturer protocols using an Automatic Biochemistry Analyzer (Modular P800, Roche Diagnostics, Basel, Switzerland).

Enzyme-Linked Immunosorbent Assay (ELISA)

After the last administration, all the rabbits were deprived of food (but not water) for 12 hours, and 1% sodium pentobarbital was injected intraperitoneally for anesthesia. Blood samples collected from the auricular vein were centrifuged at 12,000 r/min at 4 °C for 10 min to prepare the supernatant. The concentrations of CRP, IL-6 and TNF-α in the supernatant were assayed using commercially available enzyme-linked immunosorbent assay (ELISA) kits (Nanjing Jiancheng Bioengineering Institute, Nanjing, China) following the manufacturer's protocols.

Histological Analysis

The abdominal aortic tissues were excised from the rabbits, fixed in 4% paraformaldehyde for 24 h, dehydrated, and embedded in paraffin. Next, the specimens were cut into 5-μm sections, immersed in xylene twice for 5 min each at room temperature and rehydrated in 100%, 95%, 90%, 80%, 70% and 50% ethanol for 1 min each. After Masson's trichrome staining, the 5-μm sections were analyzed under a digital biological microscope (BK-DM500, Chongqing, China) to determine the collagen content of the tissue sections in plaques.

Immunohistochemistry

Immunohistochemical (IHC) staining of tissue sample slides obtained from different groups was observed under a BK-DM500 digital biological microscope, and the staining was brown and positive. The Ptps-2011 color pathological image and text analysis system was used to calculate the integrated optical density (IOD; IOD = OD × positive staining area), which was used as the immunohistochemical index of samples to represent the protein expression levels of ICAM-1, CD31 and RAM-11.

Statistical Analysis

In this study, the results from at least three independent repeats of the experiment were analyzed using GraphPad Prism 8.0 (GraphPad Software Inc., San Diego, CA, USA). The measurement data are presented as means ± SD, and the significant differences among multiple groups were evaluated by one-way analysis of variance (ANOVA). $p < 0.05$ was considered statistically significant.

Results

Screening results of Components and Target Proteins

In total, 429 components in HLJDD were obtained from the TCMSP database, 48 of which belonged to Coptidis Rhizoma, 143 to Scutellariae Radix, 140 to Phellodendri Chinensis Cortex and 98 to Gardeniae Fructus. According to the screening conditions of OB ≥30% and DL index ≥0.18, 102 components from 4 herbs of HLJDD were collected, comprising 14 (29.2%) components extracted from Coptidis Rhizoma, 36 (25.2%) from Scutellariae Radix, 37 (26.4%) from Phellodendri Chinensis Cortex, and 15 (15.3%) from Gardeniae Fructus. After removing the redundancy, 87 components were selected as candidate bioactive components, whose detailed information is shown in Table S1. After eliminating duplicates, 149 protein targets were harvested based on the target prediction performed using the SwissTargetPrediction website tool (Table S2).

Results of AS-Related Targets

For disease target identification, 4481 AS-related targets were recovered from GeneCards, and 299 targets were found from the OMIM database. After eliminating the redundant parts, 4733 correlative targets of AS were collected.

Network Construction

Of the 4733 known AS-related targets and 149 protein targets of HLJDD, 101 therapeutic candidates for AS were dug out using Venny 2.1.0 (Table 1). As described in the third step of the methods, 101 green nodes representing the therapeutic targets and 31 blue nodes representing the candidate bioactive components were utilized to construct an HLJDD–compound–target–AS network

Table 1 Common Targets Between HLJDD and AS

Target	Common Name	Uniprot ID
Myeloperoxidase	MPO	P05164
Phosphoinositide-3-Kinase Regulatory Subunit 1	PIK3R1	P27986
Adenosine A2a receptor	ADORA2A	P29274
Death Associated Protein Kinase 1	DAPK1	P53355
SRC Proto-Oncogene, Non-Receptor Tyrosine Kinase	SRC	P12931
Protein Tyrosine Kinase 2	PTK2	Q05397
Matrix metalloproteinase 13	MMP13	P45452
Matrix metalloproteinase 3	MMP3	P08254
Carbonic anhydrase III	CA3	P07451
Arachidonate 15-lipoxygenase	ALOX15	P16050
Multidrug resistance-associated protein 1	ABCC1	P33527
Matrix metalloproteinase 9	MMP9	P14780
Phosphatidylinositol-4,5-Bisphosphate 3-Kinase Catalytic Subunit Gamma	PIK3CG	P48736
Matrix metalloproteinase 2	MMP2	P08253
Protein kinase N1	PKN1	Q16512
Casein Kinase 2 Alpha 1	CSNK2A1	P68400
Arachidonate 12-lipoxygenase	ALOX12	P18054
Hepatocyte growth factor receptor	MET	P08581
CaM kinase II beta	CAMK2B	Q13554
Anaplastic Lymphoma Receptor Tyrosine Kinase	ALK	Q9UM73
AKT Serine/Threonine Kinase 1	AKT1	P31749
Cytochrome P450 1B1	CYP1B1	Q16678
Tyrosine-protein kinase receptor UFO	AXL	P30530
ATP-binding cassette sub-family G member 2	ABCG2	Q9UNQ0
Apurinic/Apyrimidinic Endodeoxyribonuclease 1	APEX1	P27695
Aldo-keto reductase family 1 member C4	AKR1C4	P17516
Aldo-Keto Reductase Family 1 Member A1	AKR1A1	P14550
Cyclin-dependent kinase 6	CDK6	Q00534
Cyclin-dependent kinase 2	CDK2	P24941
Arginase-1	ARG1	P05089
Tyrosinase	TYR	P14679
Aryl hydrocarbon receptor	AHR	P35869
Beta-galactoside alpha-2,6-sialyltransferase 1	ST6GAL1	P15907
Solute carrier family 22 member 12	SLC22A12	Q96S37
Poly [ADP-ribose] polymerase-1	PARP1	P09874
Transthyretin	TTR	P02766
Matrix metalloproteinase 12	MMP12	P39900
CD38 Molecule	CD38	P28907
Aldo-keto reductase family 1 member B10	AKR1B10	O60218
Matrix metalloproteinase 1	MMP1	P03956
Monoamine oxidase B	MAOB	P27338
C-C chemokine receptor type 2	CCR2	P41597
Forkhead box protein O1	FOXO1	Q12778
Calpain 1	CAPN1	P07384
Rat anti-rabbit macrophage antibody 11	RAM11	A5HC69
Cytochrome P450 2C9	CYP2C9	P11712
Cytochrome P450 3A4	CYP3A4	P08684
Dihydrofolate reductase	DHFR	P00374
Melanocortin receptor 4	MC4R	P32245
5-lipoxygenase activating protein	ALOX5AP	P20292
Phosphodiesterase 4B	PDE4B	Q07343

(*Continued*)

Table 1 (Continued).

Target	Common Name	Uniprot ID
Intercellular cell adhesion molecule-1	ICAM1	P05362
Acyl coenzyme A:cholesterol acyltransferase 1	SOAT1	P35610
Nuclear factor erythroid 2-related factor 2	NFE2L2	Q16236
Janus Kinase 1	JAK1	P23458
Fms Related Receptor Tyrosine Kinase 4	FLT4	P35916
Epoxide hydratase 2	EPHX2	P34913
LYN Proto-Oncogene, Src Family Tyrosine Kinase	LYN	P07948
Complement factor D	CFD	P00746
Colony Stimulating Factor 1 Receptor	CSF1R	P07333
Interleukin-1 receptor-associated kinase 4	IRAK4	Q9NWZ3
P2X purinoceptor 7	P2RX7	Q99572
Platelet endothelial cell adhesion molecule-1	CD31	P16284
Isocitrate Dehydrogenase (NADP(+)) 1	IDH1	O75874
Voltage-gated L-type calcium channel alpha-1C subunit	CACNA1C	Q13936
Tyrosine-protein kinase TIE-2	TEK	Q02763
Histone deacetylase 3	HDAC3	O15379
Histone deacetylase 6	HDAC6	Q9UBN7
Histone deacetylase 2	HDAC2	Q92769
Histone deacetylase 5	HDAC5	Q9UQL6
Heat Shock Protein 90 Alpha Family Class B Member 1	HSP90AB1	P08238
Butyrylcholinesterase	BCHE	P06276
Adrenergic receptor alpha-2	ADRA2C	P18825
Alpha-2b adrenergic receptor	ADRA2B	P18089
Muscarinic acetylcholine receptor M1	CHRM1	P11229
Cytochrome P450 2D6	CYP2D6	P10635
Histone deacetylase 7	HDAC7	Q8WUI4
Histone deacetylase 4	HDAC4	P56524
Histone deacetylase 9	HDAC9	Q9UKV0
5-Hydroxytryptamine Receptor 3A	HTR3A	P46098
Glucagon-like peptide 1 receptor	GLP1R	P43220
Cell division control protein 42 homolog	CDC42	P60953
Peptidyl-prolyl cis-trans isomerase NIMA-interacting 1	PIN1	Q13526
Lysine-specific demethylase 4C	KDM4C	Q9H3R0
Muscarinic acetylcholine receptor M3	CHRM3	P20309
Galectin-3	LGALS3	P17931
Galectin-9	LGALS9	O00182
Thymidylate synthase	TYMS	P04818
Urotensin II receptor	UTS2R	Q9UKP6
Heat Shock Protein 90 Alpha Family Class A Member 1	HSP90AA1	P07900
Epoxide hydrolase 1	EPHX1	P07099
Solute Carrier Family 1 Member 1	SLC1A1	P43005
Protein Tyrosine Kinase 2 Beta	PTK2B	Q14289
Neuropeptide Y receptor Y5	NPY5R	Q15761
Sphingosine-1-Phosphate Receptor 2	S1PR2	O95136
Lysophosphatidic Acid Receptor 2	LPAR2	P13569
Sphingosine-1-Phosphate Receptor 3	S1PR3	Q99500
Sphingosine-1-Phosphate Receptor 1	S1PR1	P21453
Platelet Derived Growth Factor Receptor Alpha	PDGFRA	P11309
Isoprenylcysteine Carboxyl Methyltransferase	ICMT	O60725
Monoglyceride Lipase	MGLL	Q99685

(Figure 1). Additionally, 101 targets and 31 constituents were linked through 445 edges, clarifying the effectiveness of HLJDD in preventing or controlling AS depending on the surgery between multiple components and their protein targets. Among these bioactive components, 4 high-degree components were associated with multiple AS targets—quercetin (degree = 42), kaempferol (degree =35), moupinamide (degree = 32) and 5-hydroxy-7-methoxy-2-(3,4,5-trimethoxyphenyl)chromone (degree = 31).

PPI Network of Common Targets

By identifying the interaction score to medium confidence, a protein–protein interaction (PPI) network of the AS-related targets was formed by the STRING database and visualized using Cytoscape. The network involved 101 nodes and 900 edges, with a 19.8 average node degree and PPI enrichment p value<1.0e-16, confirming the multitarget characteristics of HLJDD. To analyze the complex PPI network, we established network topology analysis based on three parameters—degree, MCC and EPC—to filter 11 core targets, ICAM1, CD31, RAM11, MMP9, PIK3R1, AKT1, SRC, HSP90AA1, MMP2, PTK2, and HSP90AB1 (Figure 2).

GO and KEGG Pathway Analyses

To further explore the relationship of the 101 therapeutic targets with AS, GO enrichment analysis was performed using ClueGO. The representative biological processes are illustrated in Figure 3A. The top 7 significantly enriched GO terms (adjusted p value <0.001) were positive regulation of nitric oxide biosynthetic process, epidermal growth factor receptor signaling pathway, lymphocyte costimulation, positive regulation of cyclin-dependent protein kinase activity, response to growth hormone, regulation of telomerase activity, and central nervous system neuron axonogenesis (Figure 3B). GO analysis of common targets of HLJDD and AS is showed in Figure 3C. Additionally, KEGG enrichment analysis was performed using DAVID to reveal the therapeutic mechanism underlying HLJDD in AS. Forty-four KEGG pathways were filtered with applicable thresholds p values <0.01, 20 of which with lower p values were selected for

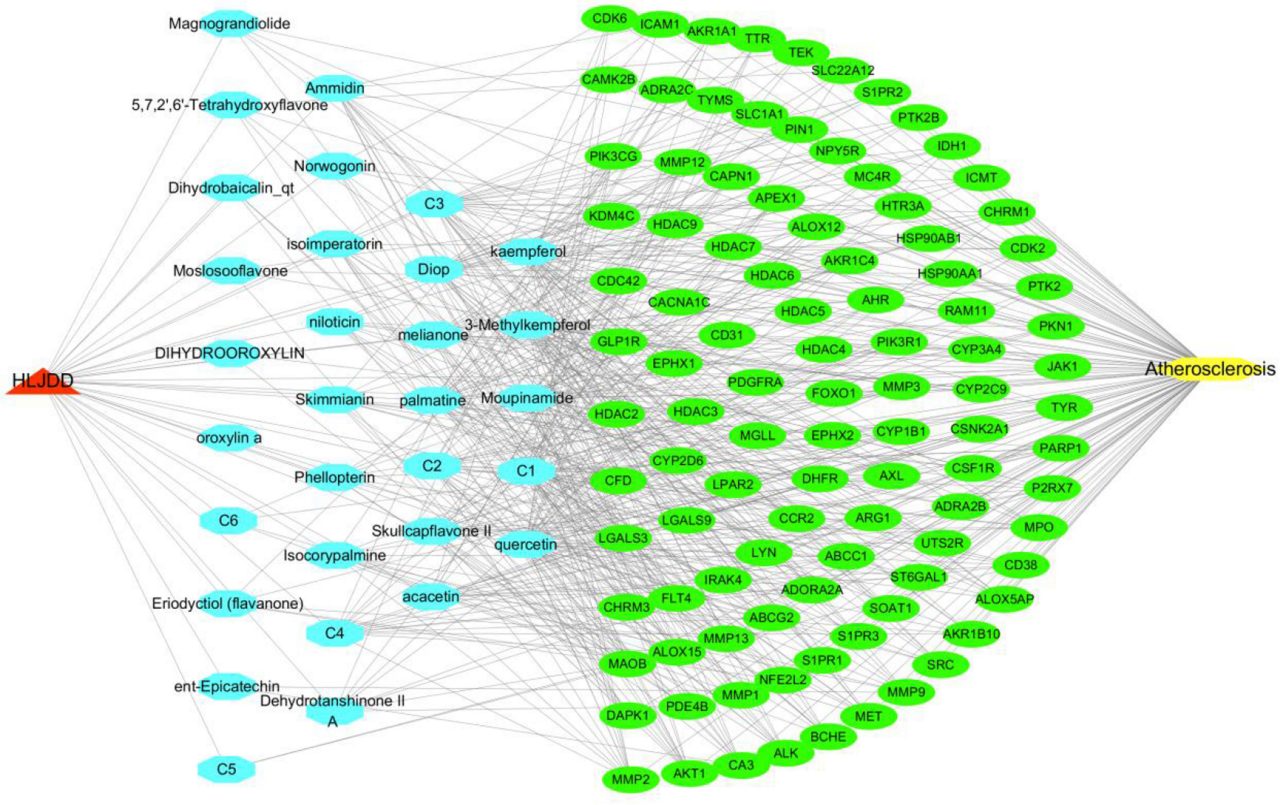

Figure 1 Network of HLJDD compound targets and AS targets.

Notes: Drug C1 represents 5-hydroxy-7-methoxy-2-(3,4,5-trimethoxyphenyl)chromone; C2 represents 5,7,2,5-tetrahydroxy-8,6-dimethoxyflavone; C3 represents bis[(2S)-2-ethylhexyl] benzene-1,2-dicarboxylate; C4 represents 5,8,2′-Trihydroxy-7-methoxyflavone; C5 represents 5,7,4′-Trihydroxy-8-methoxyflavone; C6 represents (2R)-7-hydroxy-5-methoxy-2-phenylchroman-4-one.

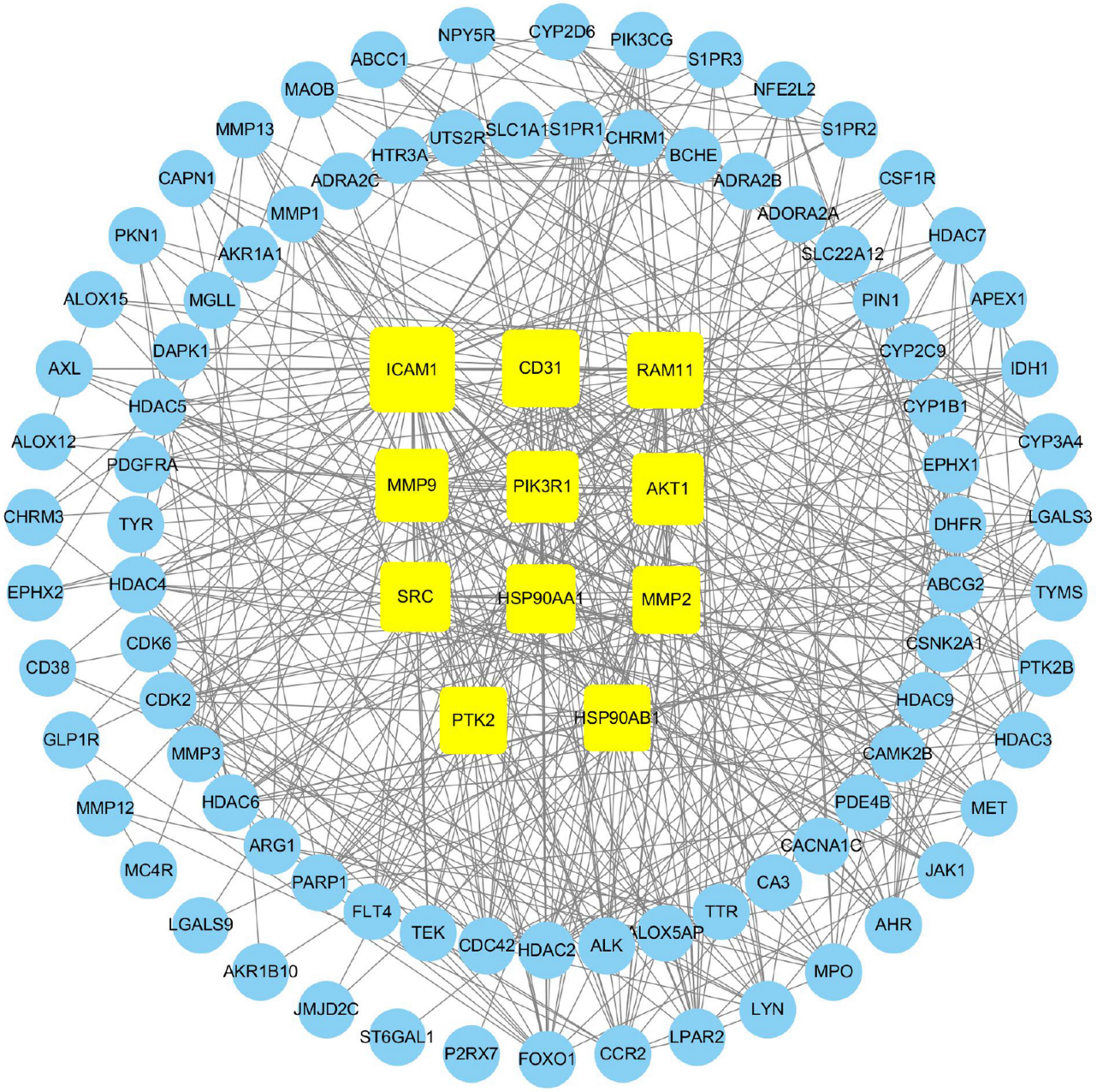

Figure 2 PPI network of common targets. The yellow squares represent the core targets. The blue circulars represent other targets.

analysis, such as platelet activation, Epstein-Barr virus infection, thyroid hormone, bacterial invasion of epithelial cells, focal adhesion, and chemokine signaling pathway (Figure 4). The enrichment analysis revealed that most of the therapeutic targets were associated with infection, cell adhesion and inflammation, suggesting that HLJDD may exert its effects against AS through anti-inflammatory effects. Based on the GO and KEGG analyses, we verified our prediction at the molecular level using network pharmacology, which predicted that ICAM1, CD31 and RAM11 were important biotargets of HLJDD in AS.

Molecular Docking Analysis

Next, molecular docking of the top 3 key targets and the 4 high-degree components were performed. It is generally believed that ligand-receptor pairs with lower-energy binding conformational stability have a higher possibility of interaction. The molecular docking results showed that the molecular docking interaction energy between the 3 key

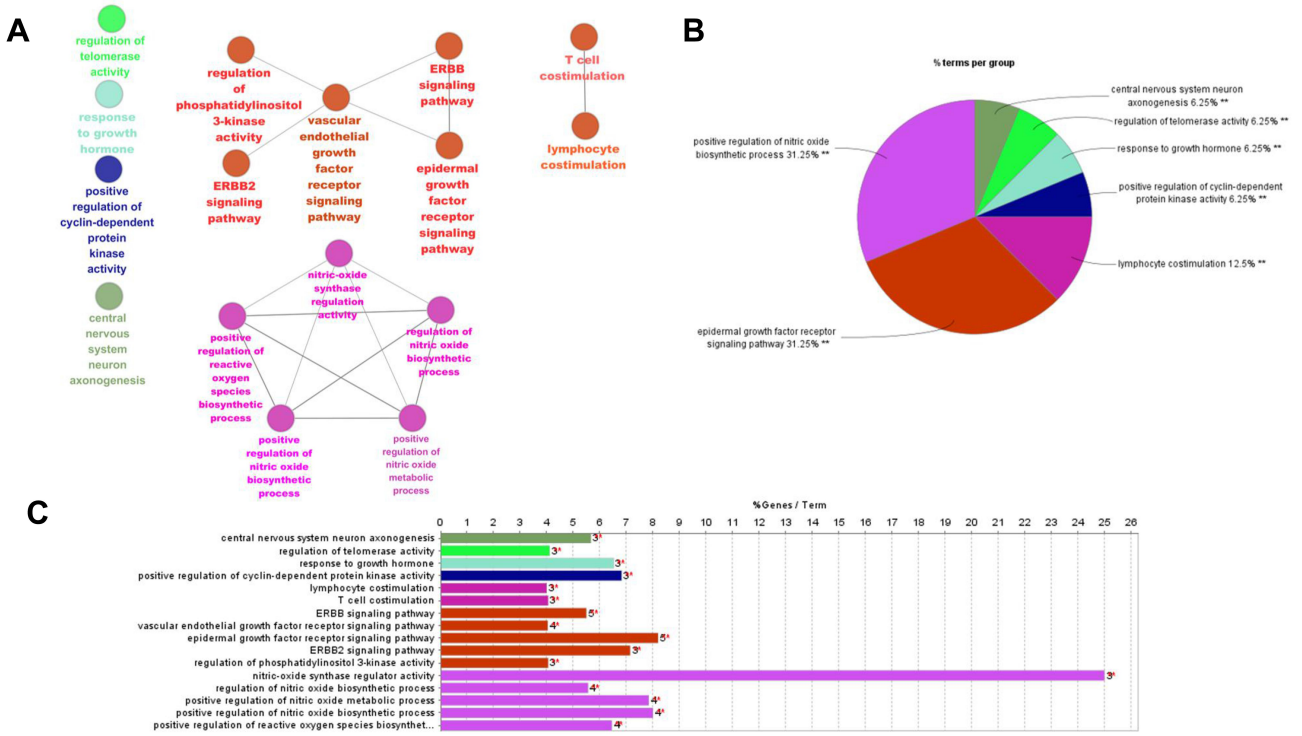

Figure 3 GO analysis. (**A**) The representative biological processes of therapeutic targets for the HLJDD against AS. The important terms in the group were tagged, with the related biological functional groups partially overlapped. (**B**) Percentage of each approach. (**C**) GO analysis of common targets of HLJDD and AS. The Y-axis represents significant GO biological function processes and the X-axis represents the counts of enriched targets.
Notes: *Adjusted *p* value <0.05, **adjusted *p* value <0.01.

targets and the 4 high-degree components were much less than −5 kJ·mol^{-1}, indicating that the 3 key targets could interact with the 4 high-degree components. The result of the molecular docking between ICAM-1 and the 4 high-degree components are presented in Figure 5.

Potential Marker Validation

Effect of HLJDD on Lipid Levels in Rabbits

Compared with those in the control group, the levels of TC, TG and LDL-C were higher in the model group, and those of HDL-C were lower (p <0.01). HLJDD significantly reduced TC, TG and LDL-C and increased HDL-C ($p < 0.05$ or 0.01) in the HLJDD and High-HLJDD groups (Figure 6).

Effects on Inflammatory Cytokines

Compared with the control group, the serum levels of CRP, IL-6 and TNF-α were significantly increased ($p <$ 0.01) in the model group. Relative to the levels in the model group, the concentrations of CRP, IL-6 and TNF-α were significantly decreased ($p < 0.05$ or 0.01) in the HLJDD and High-HLJDD groups (Figure 7A,Figure 8, Figure 9,Figure 10).

Histopathological Examination of Rabbit Aortic Tissue

Masson's trichrome staining was performed. The rabbits in the model group had collagen fibers in their ECs. By contrast, the rabbits in the control group had no collagen fibers. Compared with the model group, the rabbits in the HLJDD group had thinner collagen fibers (Figure 7B).

Immunohistochemistry Analysis

Using tissue immunofluorescence, the protein expression of ICAM-1 and RAM-11 was significantly increased ($p < 0.01$) and that of CD31 was significantly decreased ($p < 0.01$) in the model group compared with that in the control group. Additionally, ICAM-1 and RAM-11 expression was significantly downregulated ($p < 0.01$), while that of CD31 was significantly upregulated ($p <$ 0.01) in the HLJDD group at all doses (Figures 8–10).

Discussion

AS is characterized by various biological processes, including vascular injury, inflammation, oxidation of low-density lipoprotein (LDL) cholesterol, lipid deposition, cellular differentiation, and neointimal hyperplasia.[19,20]

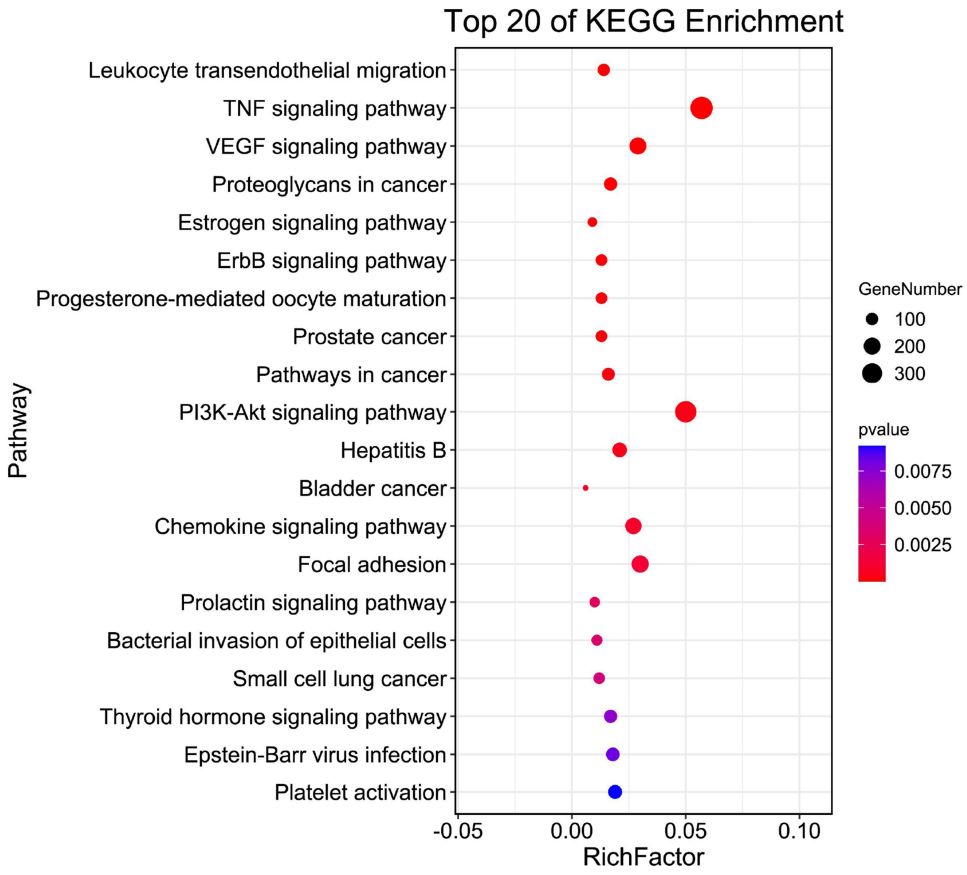

Figure 4 KEGG analysis for common targets of HLJDD and AS. The Y-axis represents significant KEGG pathways and the X-axis represents the ratio of enriched targets in a pathway to all common targets. The size of the nodes shows count of targets, and gradient of color represents the adjusted *p* value.

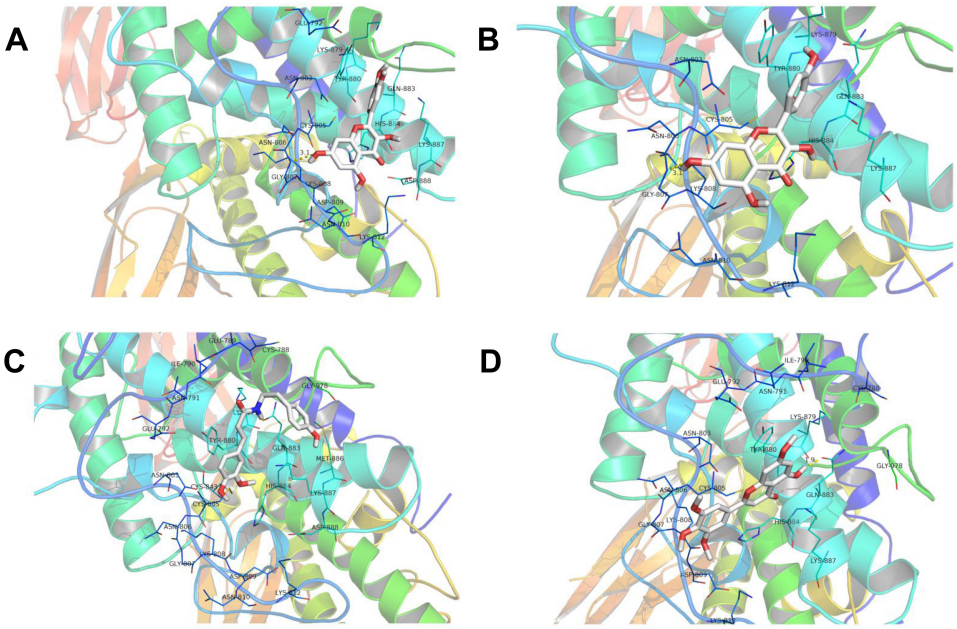

Figure 5 Molecular docking charts of quercetin and ICAM-1 (**A**), kaempferol and ICAM-1 (**B**), moupinamide and ICAM-1 (**C**), 5-hydroxy-7-methoxy-2-(3,4,5-trimethoxyphenyl)chromone and ICAM-1 (**D**).

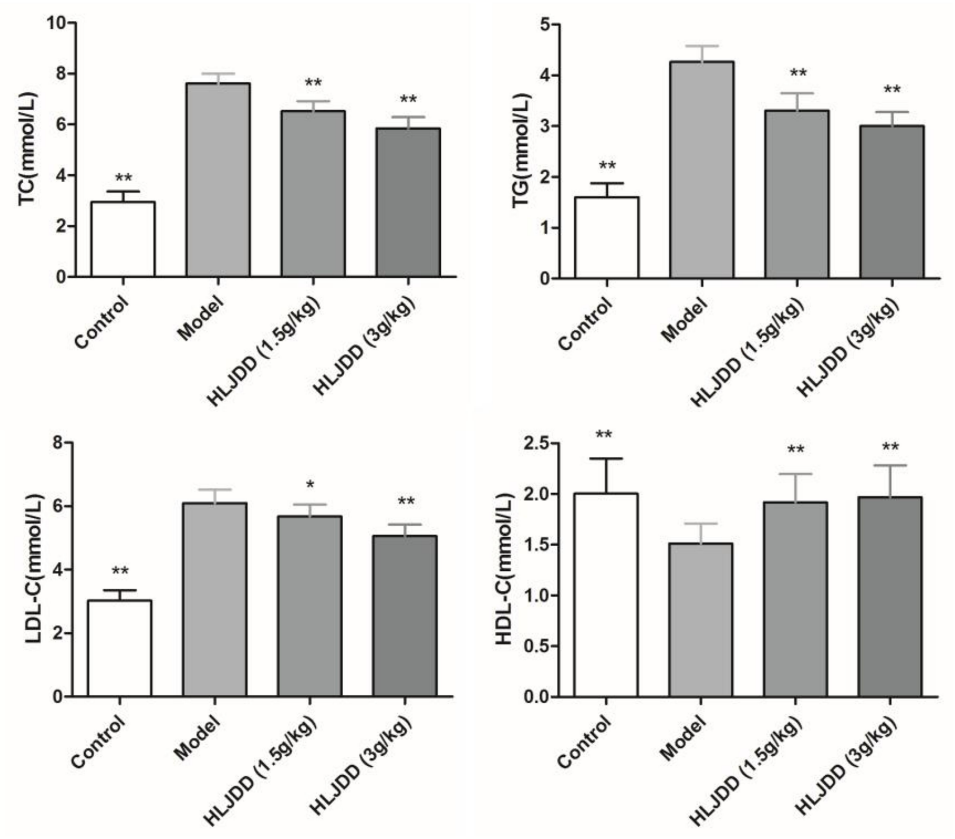

Figure 6 The TC, TG, LDL-C and HDL-C levels in rabbits.
Notes: *p<0.05 versus the model group; **p< 0.01 versus the model group. Data are the means ± SD.

AS leads to lipid accumulation, extracellular matrix protein deposition and calcification of the arterial intima and media, resulting in decreased arterial elasticity.[21] HLJDD exhibits extensive pharmacological activities with multiple targets and pathways, benefiting AS treatment. However, because of the limitations of TCM research, conducting in-depth studies on the potential mechanisms of drugs is challenging. The network pharmacology approach, which integrates systems biology and in silico technologies, is beneficial for mechanistic studies of Chinese medicine.[22] In the current study, we used this approach to confirm that HLJDD positively affects AS treatment.

In the TCM system, compounds lacking proper pharmacokinetic properties cannot reach target organs to exert biological activities. In the current study, the compounds in HLJDD with OB ≥ 30% and DL index ≥ 0.18 were considered pharmacokinetically active because they might be absorbed and distributed in the human body. Compounds with a high degree in the compound–target network may account for the major therapeutic effects of HLJDD on AS. In this study, quercetin was the most significant compound, followed by kaempferol, moupinamide and 5-hydroxy-7-methoxy-2-(3,4,5-trimethoxyphenyl)chromone. Quercetin is a dietary flavonoid compound extracted from various plants, such as apples and onions. Previous studies have revealed its anti-inflammatory, anticancer, antioxidant and anti-apoptotic activities.[23] Clinical application and pharmacological studies have found that quercetin might prevent the onset of atherosclerosis-related acute aortic syndromes through its anti-inflammatory and endothelial cell-protective effects.[24] Kaempferol is an anti-inflammatory flavonoid commonly found in plants.[25] Oxidized low-density lipoprotein (ox-LDL) induces endothelial cell (EC) apoptosis, and kaempferol was reported to alleviate ox-LDL-induced apoptosis of human umbilical vein endothelial cells and provide benefits for atherosclerosis treatment.[26] Moupinamide, also known as N-trans-feruloyltyramine (NTF), is an active phenylpropanoid compound that possesses antioxidant, antimicrobial, anti-melanogenesis and anticancer activities;[27] thus, it may affect AS treatment. 5-Hydroxy-7-methoxy-2-(3,4,5-trimethoxyphenyl)chromone, also

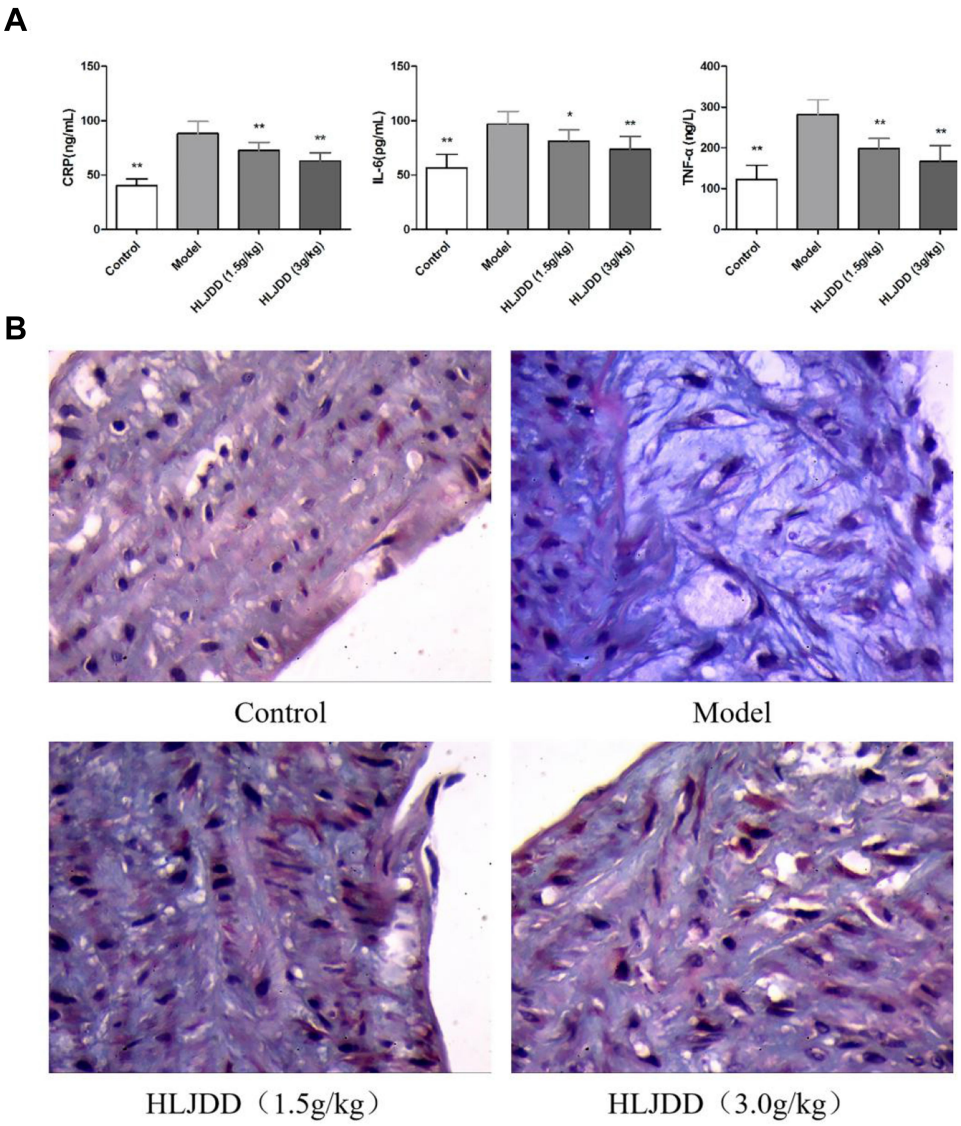

Figure 7 (**A**) The serum CRP, IL-6 and TNF-α levels in rabbits. **p*<0.05 versus the model group; ***p*< 0.01 versus the model group. Data are the means ± SD. (**B**) Representative Masson's trichrome staining of rabbit aortic tissue (×40).

called gardenin A (Gar-A), exhibits a broad spectrum of biological properties, including anticancer, antiatherogenic and neuroprotective effects.[28] Steatotic HepG2 cells treated with Gar-A showed a significant reduction in lipid accumulation concentrations in vitro. In hyperlipidemic rats, the treatment significantly reduced the lipid levels at the synthesis phase. Treatment of the animals with Gar-A significantly lowered steatosis and the transaminase levels. Other biochemical parameters, such as TC, TG, LDL-c, ALP and ACP, were also decreased significantly.[29] Treatment with Gar-A significantly lowered hyperlipidemia and fat accumulation in the liver, suggesting new options for atherosclerosis treatment.

Our network pharmacology analysis predicted that the important predictive biotargets of HLJDD in AS were ICAM-1, CD31, and RAM-11. Studies have found that the endothelial cells, intima and matrix on the arterial wall of patients with atherosclerosis all express ICAM-1. ICAM-1 is a transmembrane protein that plays an important role in innate and adaptive immune responses and is involved in the interaction between antigen-presenting cells and T cells and the migration of leukocytes through the endothelium to the site of inflammation.[30] The activation of endothelial cells mainly performed by cytokines. Some cytokines induce the expression of leukocyte and monocyte adhesion molecules on the endothelial surface, particularly intercellular adhesion

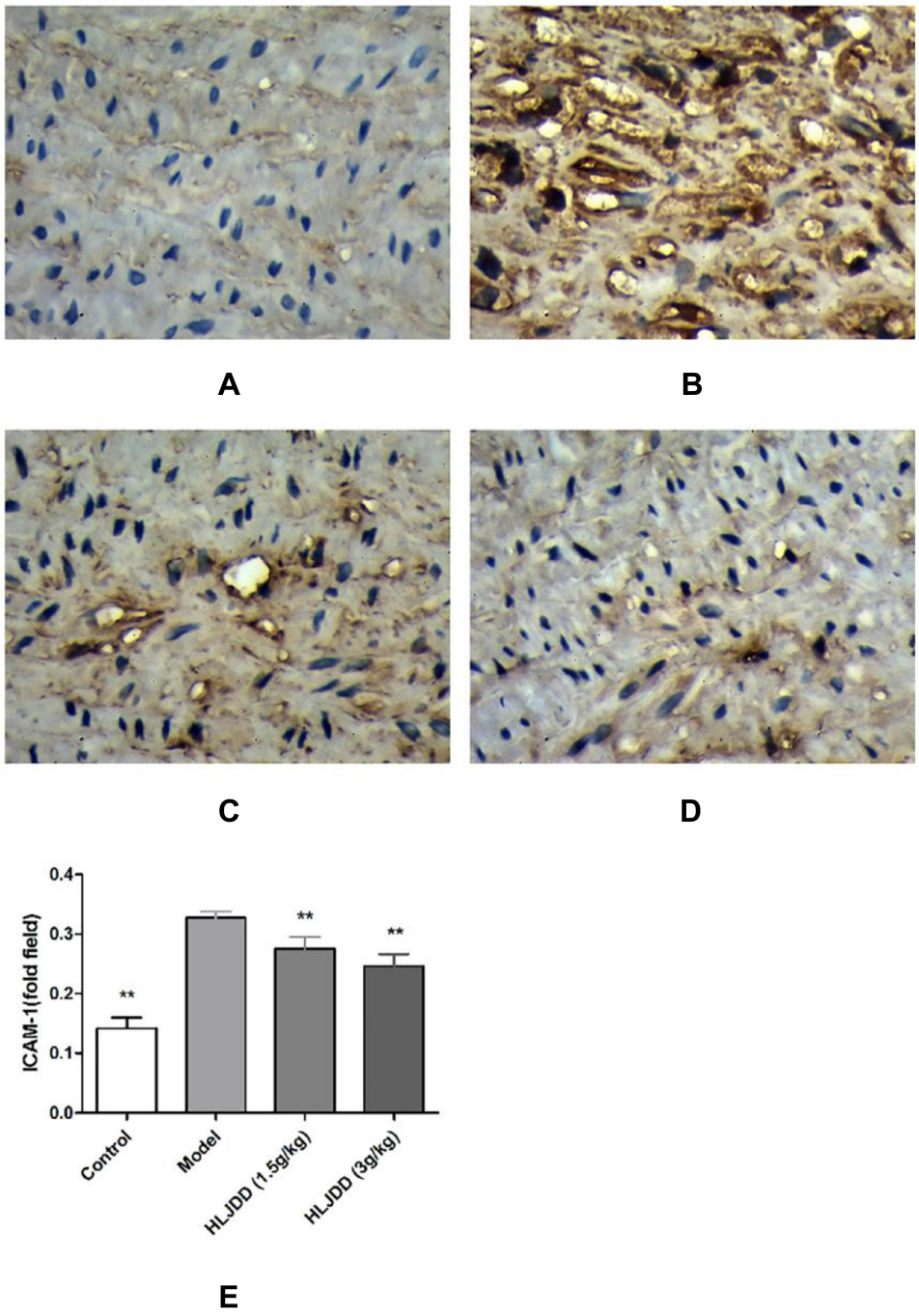

Figure 8 Effect of HLJDD on the protein expression levels of ICAM-1 (×40). (**A**) Control group (**B**) model group (**C**) HLJDD (1.5g/kg) group (**D**) HLJDD (3g/kg) group. (**E**) The integrated optical density of ICAM-1 was calculated by Ptps-2011 software.
Notes: $^{**}p < 0.01$ versus the model group.

molecules. Monocytes and T lymphocytes accumulate in the lining of blood vessel walls mediated by these adhesion molecules. Specific chemokines cause smooth muscle cells to migrate from the culture medium to the inner membrane, and then cell proliferation occurs.[31] The only constitutively expressed factor in vascular interface cells is the transhomophilic inhibitory immune receptor CD31, which may play an important role in vascular homeostasis. Notably, experiments have shown that CD31 signal transduction prevents blood adhesion, chronic inflammatory diseases and platelet

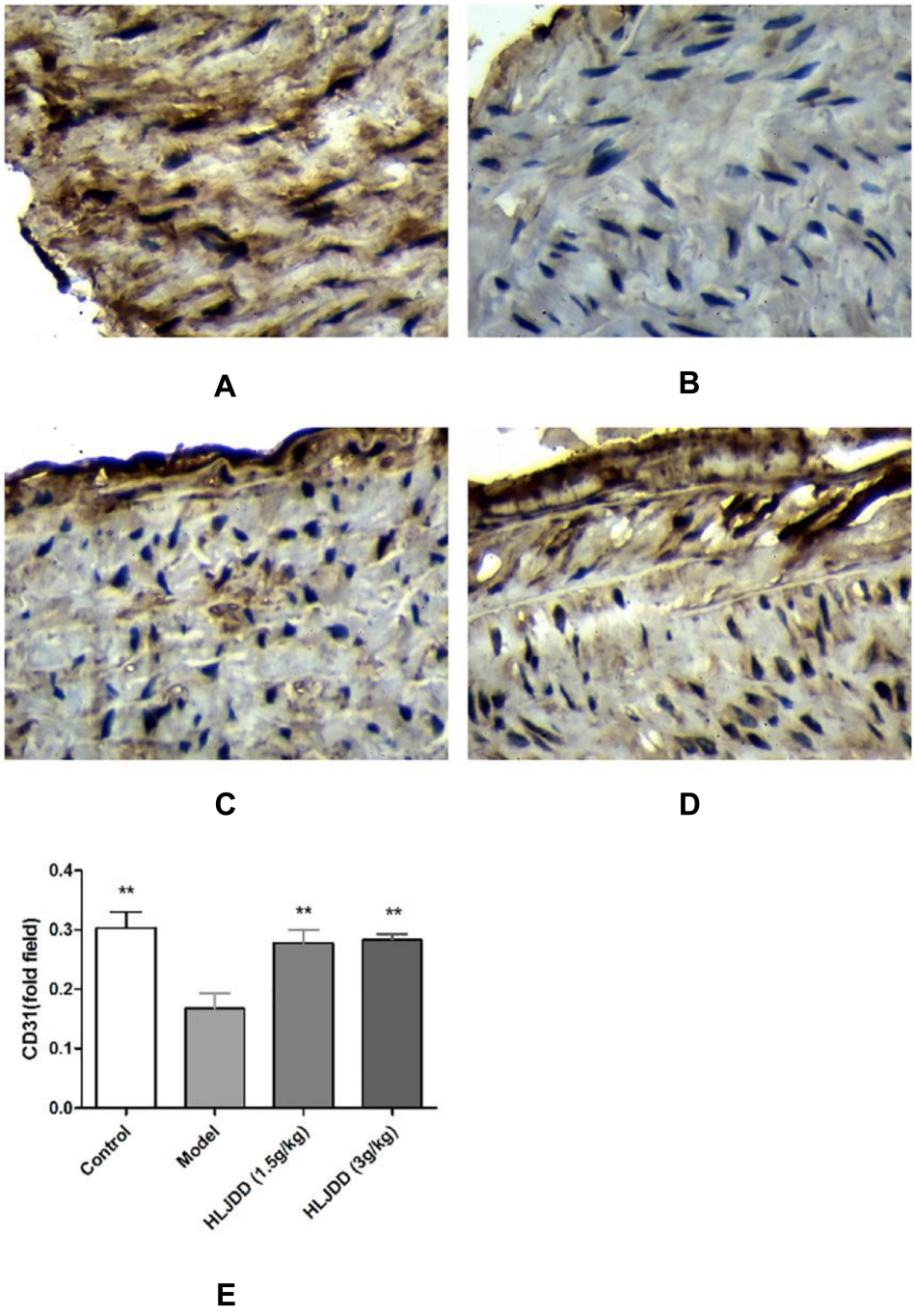

Figure 9 Effect of HLJDD on the protein expression levels of CD31 (×40). (**A**) Control group (**B**) model group (**C**) HLJDD (1.5g/kg) group (**D**) HLJDD (3g/kg) group. (**E**) The integrated optical density of CD31 was calculated by Ptps-2011 software.
Notes: $^{**}p < 0.01$ versus the model group.

thrombosis.[32] CD31 shows unique cross-affinity and receptor co-signaling properties; thus, it can coordinate the cross-reaction of biomechanics, metabolism and inflammatory stimuli to exert cell-specific effects. CD31 is at the center of mediating mechanical, metabolic and immunological changes and provides a single target with beneficial pleiotropic effects in the cardiovascular system.[33] RAM-11 and HIF-1α are highly positively correlated, and the target genes regulated by HIF-1α are involved in cell proliferation, differentiation and survival. Smooth muscle cells and macrophages play important roles in the formation and development of AS. Additionally, they secrete vascular growth

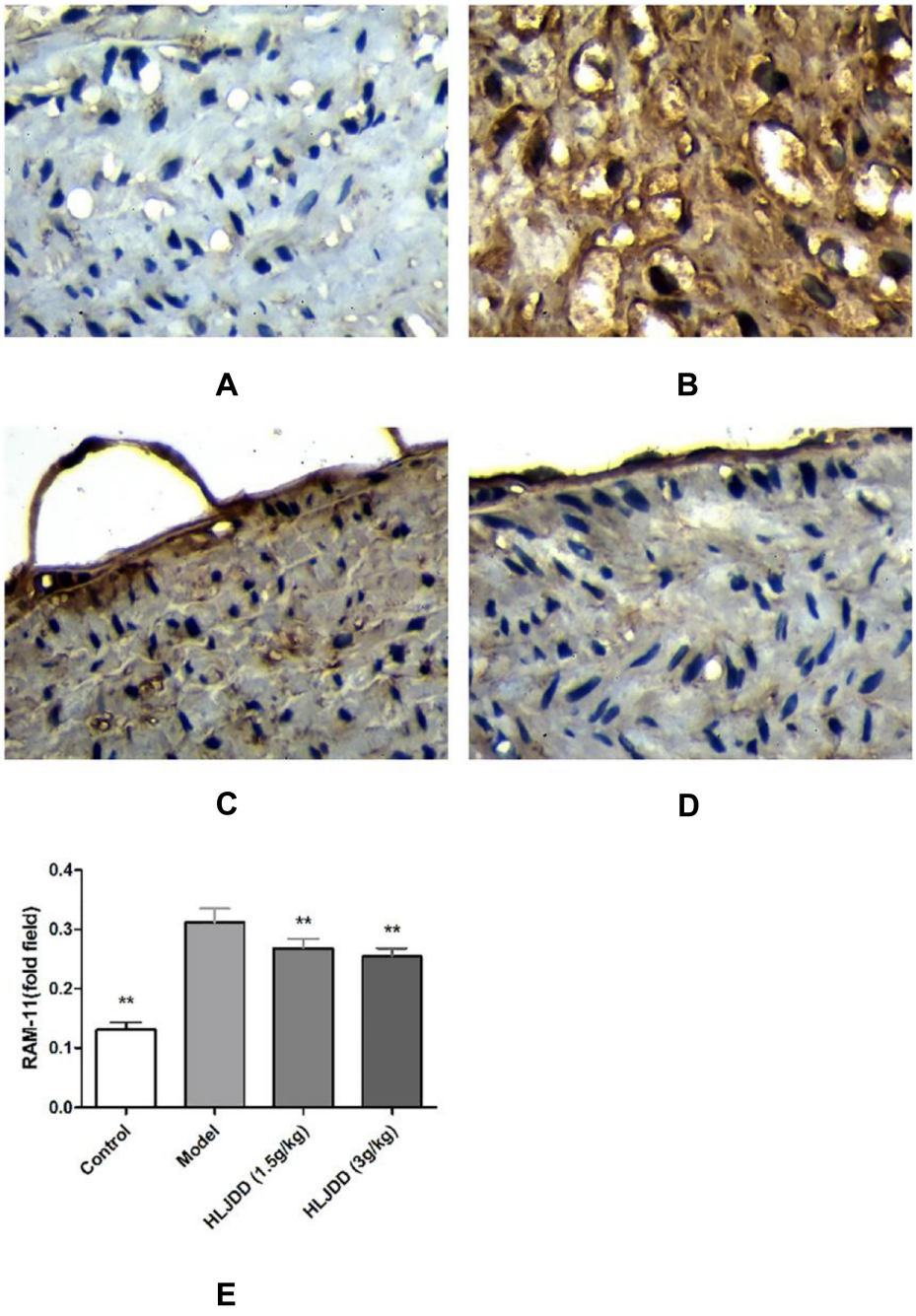

Figure 10 Effect of HLJDD on the protein expression levels of RAM-11 (×40). (**A**) Control group (**B**) model group (**C**) HLJDD (1.5g/kg) group (**D**) HLJDD (3g/kg) group. (**E**) The integrated optical density of RAM-11 was calculated by Ptps-2011 software.
Notes: $^{**}p < 0.01$ versus the model group.

factors and decompose the basement membrane to promote new blood vessel formation in AS. Studies have shown that HIF-1α is involved in the infiltration and activation of macrophages and smooth muscle cell migration and proliferation in AS lesions, thereby promoting new blood vessel formation in plaques, a key event in AS lesions.[34]

The KEGG results indicated that HLJDD regulates leukocyte transendothelial migration as the pharmacological mechanism of the therapeutic effect of HLJDD against AS. Inflammation is tightly regulated by the body and associated with the transient crossing of leukocytes through the blood vessel wall, a process called

transendothelial migration (TEM) or diapedesis.[35] TEM is one of the crucial steps during inflammation.[36] Pro-inflammatory cytokines are synthesized and secreted into the blood following over-activation of the NF-κB signaling pathway, causing oxidative stress and inflammation that result in endothelial cell damage. The adhesion molecule ICAM-1 is a central mediator of TEM, and interfering with ICAM-1 is sufficient to block transmigration.[35,36] The high expression of ICAM-1 and other adhesion molecules further promotes the adhesion and migration of monocytes in the early stage of atherosclerosis. A reduced expression of ICAM-1 inhibits the migration and adhesion of monocytes, antagonizing proliferation in atherosclerotic vessels.[21] TEM involves an orchestrated series of events within endothelial cells to facilitate the passage of leukocytes while maintaining tight apposition to prevent plasma leakage.[35] Thus, targeting leukocyte transendothelial migration may be a potential therapeutic approach for AS.

In the present study, we investigated the impact of HLJDD on AS development by establishing hypercholesterolemic rabbit models fed a high-fat diet. The results reflected that HLJDD might treat AS mainly by reducing TC, TG and LDL-C and increasing HDL-C, upregulating CD31 expression, reducing ICAM-1 and RAM-11 expression, and downregulating inflammatory factors, including CRP, IL-6 and TNF-α. These results support the network pharmacology data and demonstrate that HLJDD affects the expression of core genes and alters the leukocyte transendothelial migration signaling pathway.

In conclusion, the pharmacological mechanism by which HLJDD-treated AS was investigated by combining network pharmacology prediction and experimental validation. The core targets identified included ICAM-1, CD31 and RAM-11 in the network of HLJDD and AS, and we demonstrated that HLJDD might affect AS mainly by upregulating CD31 expression and reducing ICAM-1 and RAM-11 expression. Moreover, leukocyte transendothelial migration plays an important regulatory role in the mechanism of HLJDD in AS treatment. This study has some drawbacks that require further research, which include the need for in-depth study on bioactive components and further experimental validation to verify the effect of the HLJDD on AS. However, this study confirmed the feasibility of exploring AS treatment using the classical prescription of HLJDD based on network pharmacology.

Funding

This work was supported by National Natural Science Foundation of China (81673923), Foundation for scientific research platforms and projects in Higher Education of Guangdong Province in China (2018KQNCX038), and Incubation of Innovative Program of First Clinical Medical College of Guangzhou University of Chinese Medicine (2018XXDT01).

Disclosure

The authors declare that there are no conflicts of interest.

References

1. Benjamin EJ, Muntner P, Alonso A, et al.; American Heart Association Council on Epidemiology and Prevention Statistics Committee and Stroke Statistics Subcommittee. Heart disease and stroke statistics-2019 update: a report from the American Heart Association. *Circulation*. 2019;139(10):e56–e528. doi:10.1161/CIR.0000000000000659
2. Arnett DK, Blumenthal RS, Albert MA, et al. 2019 ACC/AHA guideline on the primary prevention of cardiovascular disease: a report of the American College of Cardiology/American Heart Association Task Force on Clinical Practice Guidelines. *Circulation*. 2019;140(11):e596–e646. doi:10.1161/CIR.0000000000000678
3. Oshima T, Miwa H, Joh T. Aspirin induces gastric epithelial barrier dysfunction by activating p38 MAPK via claudin-7. American journal of physiology. *Cell Physiol*. 2008;295(3):C800–C806. doi:10.1152/ajpcell.00157.2008
4. Shen L, Shah BR, Reyes EM, et al. Role of diuretics, β blockers, and statins in increasing the risk of diabetes in patients with impaired glucose tolerance: reanalysis of data from the NAVIGATOR study. *BMJ*. 2013;347:f6745. doi:10.1136/bmj.f6745
5. Singh RB, Mengi SA, Xu YJ, Arneja AS, Dhalla NS. Pathogenesis of atherosclerosis: a multifactorial process. *Exp Clin Cardiol*. 2002;7(1):40–53.
6. Jiang L, Xiong Y, Yu L, et al. Simultaneous determination of seven active components in rat plasma by UHPLC-MS/MS and application to a quantitative study after oral administration of Huang-Lian Jie-Du Decoction in high fat-induced atherosclerosis rats. *Int J Anal Chem*. 2019;2019:5628160. doi:10.1155/2019/5628160
7. Fang X.Research progress on pharmacological effects of Huanglian Jiedu Decoction. *Chin Trad Patent Med*. 2015;37(10):2254–2259.
8. Li T, Han J, Wang B, et al.Huanglian jiedu decoction regulated and controlled differentiation of monocytes, macrophages, and foam cells: an experimental study. *Chin J Integr Trad West Med*. 2014;34(09):1096–1102.
9. Ma YM, Zhang XZ, Su ZZ, et al. Insight into the molecular mechanism of a herbal injection by integrating network pharmacology and in vitro. *J Ethnopharmacol*. 2015;173:91–99. doi:10.1016/j.jep.2015.07.016
10. Cui Y, Li C, Zeng C, et al. Tongmai Yangxin pills anti-oxidative stress alleviates cisplatin-induced cardiotoxicity: network pharmacology analysis and experimental evidence. *Biomed Pharmacother*. 2018;108:1081–1089. doi:10.1016/j.biopha.2018.09.095
11. Luo TT, Lu Y, Yan SK, Xiao X, Rong XL, Guo J. Network pharmacology in research of chinese medicine formula: methodology, application and prospective. *Chin J Integr Med*. 2020;26(1):72–80. doi:10.1007/s11655-019-3064-0

12. Ru J, Li P, Wang J, et al. TCMSP: a database of systems pharmacology for drug discovery from herbal medicines. *J Cheminform*. 2014;6:13. doi:10.1186/1758-2946-6-13
13. Stelzer G, Rosen N, Plaschkes I, et al. The genecards suite: from gene data mining to disease genome sequence analyses. *Curr Protocols Bioinform*. 2016;54:1.30.1–1.30.33. doi:10.1002/cpbi.5
14. Amberger JS, Hamosh A. Searching Online Mendelian Inheritance in Man (OMIM): a knowledgebase of human genes and genetic phenotypes. *Curr Protocols Bioinform*. 2017;58:1.2.1–1.2.12. doi:10.1002/cpbi.27
15. Oliveros JCV. An interactive tool for comparing lists with venn diagrams; 2021. Available from: https://bioinfogp.cnb.csic.es/tools/venny/index.html. Accessed April 19, 2021.
16. Shannon P, Markiel A, Ozier O, et al. Cytoscape: a software environment for integrated models of biomolecular interaction networks. *Genome Res*. 2003;13(11):2498–2504. doi:10.1101/gr.1239303
17. Szklarczyk D, Morris JH, Cook H, et al. The STRING database in 2017: quality-controlled protein-protein association networks, made broadly accessible. *Nucleic Acids Res*. 2017;45(D1):D362–D368. doi:10.1093/nar/gkw937
18. Fan J, Chen Y, Yan H, Niimi M, Wang Y, Liang J. Principles and applications of rabbit models for atherosclerosis research. *J Atheroscler Thromb*. 2018;25(3):213–220. doi:10.5551/jat.RV17018
19. Sato Y, Watanabe R, Uchiyama N, et al. Inhibitory effects of vasostatin-1 against atherogenesis. *Clin Sci*. 2018;132(23):2493–2507. doi:10.1042/CS20180451
20. Herrington W, Lacey B, Sherliker P, Armitage J, Lewington S. Epidemiology of atherosclerosis and the potential to reduce the global burden of atherothrombotic disease. *Circ Res*. 2016;118(4):535–546. doi:10.1161/CIRCRESAHA.115.307611
21. Wu Y, Wang Y, Liu X, et al. Ziziphora clinopodioides flavonoids based on network pharmacology attenuates atherosclerosis in rats induced by high-fat emulsion combined with vitamin D_3 by down-regulating VEGF/AKT/NF-κB signaling pathway. *Biomed Pharmacother*. 2020;129:110399. doi:10.1016/j.biopha.2020.110399
22. Guo W, Huang J, Wang N, et al. Integrating network pharmacology and pharmacological evaluation for deciphering the action mechanism of herbal formula Zuojin pill in suppressing hepatocellular carcinoma. *Front Pharmacol*. 2019;10:1185. doi:10.3389/fphar.2019.01185
23. Lu XL, Zhao CH, Yao XL, Zhang H. Quercetin attenuates high fructose feeding-induced atherosclerosis by suppressing inflammation and apoptosis via ROS-regulated PI3K/AKT signaling pathway. *Biomed Pharmacother*. 2017;85:658–671. doi:10.1016/j.biopha.2016.11.077
24. Kondo M, Izawa-Ishizawa Y, Goda M, et al. Preventive effects of quercetin against the onset of atherosclerosis-related acute aortic syndromes in mice. *Int J Mol Sci*. 2020;21(19):7226. doi:10.3390/ijms21197226
25. Tu YC, Lian TW, Yen JH, Chen ZT, Wu MJ. Antiatherogenic effects of kaempferol and rhamnocitrin. *J Agric Food Chem*. 2007;55(24):9969–9976. doi:10.1021/jf0717788
26. Zhong X, Zhang L, Li Y, Li P, Li J, Cheng G. Kaempferol alleviates ox-LDL-induced apoptosis by up-regulation of miR-26a-5p via inhibiting TLR4/NF-κB pathway in human endothelial cells. *Biomed Pharmacother*. 2018;108:1783–1789. doi:10.1016/j.biopha.2018.09.175
27. Jiang Y, Yu L, Wang MH. N-trans-feruloyltyramine inhibits LPS-induced NO and PGE2 production in RAW 264.7 macrophages: involvement of AP-1 and MAP kinase signalling pathways. *Chem Biol Interact*. 2015;235:56–62. doi:10.1016/j.cbi.2015.03.029
28. Chiu SP, Wu MJ, Chen PY, et al. Neurotrophic action of 5-hydroxylated polymethoxyflavones: 5-demethylnobiletin and gardenin A stimulate neuritogenesis in PC12 cells. *J Agric Food Chem*. 2013;61(39):9453–9463. doi:10.1021/jf4024678
29. Toppo E, Darvin SS, Esakkimuthu S, et al. Antihyperlipidemic and hepatoprotective effects of Gardenin A in cellular and high fat diet fed rodent models. *Chem Biol Interact*. 2017;269:9–17. doi:10.1016/j.cbi.2017.03.013
30. Lawson C, Wolf S. ICAM-1 signaling in endothelial cells. *Pharmacol Pep*. 2009;61(1):22–32. doi:10.1016/s1734-1140(09)70004-0
31. Malekmohammad K, Sewell R, Rafieian-Kopaei M. Antioxidants and atherosclerosis: mechanistic aspects. *Biomolecules*. 2019;9(8):301. doi:10.3390/biom9080301
32. Fornasa G, Clement M, Groyer E, et al. A CD31-derived peptide prevents angiotensin II-induced atherosclerosis progression and aneurysm formation. *Cardiovasc Res*. 2012;94(1):30–37. doi:10.1093/cvr/cvs076
33. Caligiuri G. Mechanotransduction, immunoregulation, and metabolic functions of CD31 in cardiovascular pathophysiology. *Cardiovasc Res*. 2019;115(9):1425–1434. doi:10.1093/cvr/cvz132
34. Wu M, He W, Zhao H, et al. HIF-1α and neovascularization in early carotid atherosclerosis plaques in rabbits. *Zhong Nan Da Xue Xue Bao Yi Xue Ban*. 2010;35(10):1057–1063. doi:10.3969/j.issn.1672-7347.2010.10.005
35. Muller WA. Mechanisms of leukocyte transendothelial migration. *Annu Rev Pathol*. 2011;6:323–344. doi:10.1146/annurev-pathol-011110-130224
36. Heemskerk N, van Rijssel J, van Buul JD. Rho-GTPase signaling in leukocyte extravasation: an endothelial point of view. *Cell Adh Migr*. 2014;8(2):67–75. doi:10.4161/cam.28244